

Microbial solubilization of silicon and phosphorus from bedrock in relation to abundance of phosphorus-solubilizing bacteria in temperate forest soils

Giovanni Pastore^a, Sarmite Kernchen^b, Marie Spohn^{a,c,*}

^a Department of Soil Biogeochemistry, Bayreuth Center of Ecology and Environmental Research (BayCEER), University of Bayreuth, Germany

^b Atmospheric Chemistry, University of Bayreuth, Germany

^c Biogeochemistry of Forest Soils, Swedish University of Agricultural Sciences, Uppsala, Sweden

ARTICLE INFO

Keywords:

Biogenic rock weathering
Silicate weathering
P-solubilizing bacteria
Phosphorus solubilization
Silicon solubilization
Organic acids

ABSTRACT

Biogeochemical weathering of bedrock is the most important input of silicon (Si) and phosphorus (P) to forest ecosystems. While soil microbes, and in particular P-solubilizing bacteria (PSB), are known to accelerate the solubilization of Si and P from silicate rocks, our understanding of the mechanisms driving biogenic weathering are still limited. To fill this gap, incubation experiments with weathered parent materials (i.e. basalt, andesite and paragneiss) of four soils and water extracts of the four soils, differing in P stocks, were conducted. We found that the net Si solubilization rate ranged from 5.0 (± 1.8) to 91.0 (± 2.4) nmol m⁻² d⁻¹ across all examined soils. The silicate dissolution rates were negatively related to the decrease in pH (Δ pH) and positively related to the amounts of organic acids released by microbes. We found that the gross P solubilization rates from the parent materials were ~11 times higher at the P-rich site (BBR) compared to the P-poor site (CON). In addition, we determined the abundance and the taxonomic composition of PSB communities in the four soils. The abundance of PSB ranged from 2% at the P-rich site to 22.1% at the P-poor site, indicating that a selective pressure exists in P-poor soils towards a higher abundance of P-solubilizers. Yet, despite the relative high abundance of PSB, the gross P solubilization rates were low in the soils derived from P-poor parent material. The genus *Pseudomonas* was found only in the PSB community at the P-poor site. *Burkholderiales* and *Bacillales* together were by far the two most abundant orders among the PSB communities in all soils and depths. In conclusion, this study shows that PSB are more abundant in P-poor soil than in P-rich soil, while the weathering rate seems to be mostly dependent on the bedrock.

1. Introduction

Phosphorus (P) plays a significant role for a broad array of cellular processes of all organisms (Malhotra et al., 2018). However, only a very limited proportion of P in soils is directly available to plants and microbes (Zhu et al., 2011). Therefore, P is a key factor that limits plant growth in many areas of the world (Ågren et al., 2012). Microorganisms are known to play a major role in the dissolution of minerals (Banfield et al., 1999; Vorhies and Gaines, 2009). Various studies have shown that P-solubilizing bacteria (PSB) can constitute up to 53% of total bacterial numbers and can convert insoluble forms of P to accessible ones (Browne et al., 2009). Among them, bacterial strains of the genus *Pseudomonas*, *Burkholderia*, *Erwinia*, *Enterobacter* and *Klebsiella* have been reported to be efficient P solubilizers (Chung et al., 2005; Oteino

et al., 2015; Lee et al., 2019).

P mobilization from organic matter (i.e. P mineralization) has been comprehensively explored in many studies (Zou et al., 1992; Achat et al., 2010; Spohn and Kuzyakov, 2013; Bünemann, 2015). In contrast, microbial P solubilization from silicate parent materials is not fully understood yet. The term P solubilization refers to desorption of adsorbed P as well as dissolution of P-containing minerals (Hinsinger, 2001; Penn and Camberato, 2019). In soils, P largely derives from apatites dissolution, while other nutrients become mostly available from silicate weathering (Harley and Gilkes, 2000). Although much knowledge has been gained over the past decades, the processes involved in biogenic weathering and the role of soil microbial communities are not yet fully understood (White and Brantley, 2003; Brucker et al., 2020). Bacteria and fungi are capable to secrete different compounds (e.g., organic

* Corresponding author. Department of Soil Biogeochemistry, Bayreuth Center of Ecology and Environmental Research (BayCEER), University of Bayreuth, Germany.

E-mail address: marie.spohn@slu.se (M. Spohn).

<https://doi.org/10.1016/j.soilbio.2020.108050>

Received 12 May 2020; Received in revised form 13 October 2020; Accepted 15 October 2020

Available online 16 October 2020

0038-0717/© 2020 The Authors. Published by Elsevier Ltd. This is an open access article under the CC BY license (<http://creativecommons.org/licenses/by/4.0/>).

acids; siderophores) that may affect the solubilization of P and other nutrients from rocks in three principal ways: (i) through binding (complexation) of carboxylic (-COOH) and hydroxyl (-OH) groups to metal cations (Al, Fe, Ca), (ii) through exchange of organic compounds and sorbed P (ligand exchange) and (iii) by acidification of the soil solution which causes dissolution since the dissolution of silicates and apatites is largely dependent on pH (Lindsay, 1979; Kpombekou and Tabatabai, 1994; Welch et al., 2002; Oburger et al., 2011; Wang et al., 2016).

Primary P-rich minerals such as apatites, $\text{Ca}_5(\text{PO}_4)_3(\text{OH}, \text{F}, \text{Cl})$, are present as small inclusions in nearly all silicates. Silicates compose more than 90 percent of Earth's crust and are found as major constituents of most igneous, sedimentary and metamorphic rocks (for a review see White and Brantley, 1995). Igneous rocks contain on average a higher proportion of apatite than metamorphic and sedimentary rocks (Syers et al., 1967; Bacon and Brown, 1992; Nezat et al., 2007; Mehmood et al., 2018). Thus, one would expect a higher release of P from rocks having a higher content of apatite-P. The crystallographic arrangement of silicate minerals is centered around the silicon-oxygen tetrahedron group (SiO_4^{4-}). Silica tetrahedra contains void spaces that are occupied by various metal cations to maintain electrical neutrality (Huang and Wang, 2005). Contrary to P, silicon (Si) is not considered essential for plant growth, although several studies have proven its favorable effects on growth and disease resistance in many crops (Ma, 2004; Guntzer et al., 2012; Duboc et al., 2019). In soils, the content of bioavailable Si varies from 0.003 to 0.45 g Si kg^{-1} (Liang et al., 2015), whereas bioavailable P varies from 0.02 to 0.1 g P kg^{-1} (Yang and Post, 2011). Biogenic silicate weathering can be caused by the same mechanisms as apatite weathering (Uroz et al., 2009; Brucker et al., 2020). In addition, the Si concentration in soil is affected by Si sorption/desorption (Haynes and Zhou, 2020). However, the extent to which microorganisms, and in particular PSB, impact the solubilization rate of silicate minerals is far from being completely understood.

The rates of silicate solubilization by microbial consortia differ depending on the type of parent material and soil properties (Vandevivere et al., 1994; Rogers and Bennett, 2004). Some authors (Gleeson et al., 2006; Uroz et al., 2015) suggested that rocks and soils influence the composition of the microbial communities according to their mineralogy, nutrient content and weatherability. For example, Nicolitch et al. (2016) showed that PSB were significantly more abundant in nutrient-poor than in nutrient-rich soils, but this analysis was limited to the rhizosphere and no rates of P and Si solubilization were determined. To the best of our knowledge, only one study investigated the relationship between the P solubilization rates from weathered bedrocks and the PSB communities together, so far (Spohn et al., 2020). The authors found that P solubilization was higher in moderately-weathered than in strongly-weathered saprolite and that the abundance of PSB was increased in the strongly-weathered saprolite (Spohn et al., 2020).

The principal aim of this study was to examine microbial solubilization of Si and P from different silicate parent materials (i.e. basalt, andesite and paragneiss) in four beech forest soils differing in total P stocks. A second objective was to explore the relationship between the abundance and the community composition of soil PSB and the Si and P solubilization rates. We hypothesized that (i) the rates of biogenic Si and P solubilization from weathered silicate parent materials are correlated with the concentrations of organic acids and protons released by microorganisms; (ii) the rates of microbial P solubilization from silicate parent materials increase with decreasing crystallinity of the parent material since silicates with a high content of Si (paragneiss) tend to weather more slowly than silicates having less Si (basalt, andesite) and (iii) the abundance of PSB increases with decreasing P stocks of the soils. To test these hypotheses, we performed an experiment in which we determined the solubilization of Si and P from four silicate parent materials incubated with soil extracts. Two depth increments were chosen to gain a more complete insight into microbial Si and P solubilization. In each soil extract incubated with the corresponding parent material, the

amounts of organic acids and the pH were recorded at different time points during the incubation. In addition, we determined the abundance and the taxonomy of soil PSB based on a physiological assay in combination with 16s rRNA gene sequencing.

2. Materials and methods

2.1. Study sites and sample collection

Soil samples and weathered silicate parent materials were collected in April 2017 from four even-aged beech (*Fagus sylvatica* L.) forests in Germany (Table 1). Two sites (Mitterfels, MIT and Conventwald, CON) are located on the German southern uplands and two (Bad Brückenau, BBR and Vessertal, VES) on the central uplands encompassing an altitudinal range from 810 to 1025 m above sea level. The mean annual temperatures (MAT) in the four studied sites vary from 4.5 °C at MIT to 6.8 °C at CON, whereas the mean annual precipitations (MAP) vary from 1031 mm at BBR to 1749 mm at CON. The soils of the four study sites are classified as Cambisols (WRB 2015) as described in Lang et al. (2017). The pH of the studied soils ranged from 4.5 to 5.1. The soil texture is shown in Table S2. In each forest stand, the mineral soil was sampled at two depths (30–35 cm and 65–70 cm) from one representative soil pit by combining material taken from five randomly selected spots per depth using small stainless steel spatulas. Silicate parent materials were collected from each soil depth and placed into plastic bags. After being transported to the laboratory, field-moist soil samples were sieved (<2 mm) and root fragments as well as other coarse debris were removed. Subsequently, small aliquots of each soil sample were air-dried for chemical analysis. The remaining soil was stored at (i) 5 °C for the incubation experiments or (ii) frozen at -20 °C for the microbial analysis.

2.2. Sample preparation

Parent materials were crushed using a jaw crusher (Pulverisette, Fritsch, Germany). Each crushed sample was initially sieved through a 0.63 mm sieve. The resulting size fraction was further sieved through a 0.2 mm sieve. The material that did not pass the latter was used for the incubation experiments (0.2–0.63 mm size fraction). The specific surface area (SSA) of each crushed rock was determined by N_2 adsorption on a micromeritics automatic analyzer (Gemini 2375, Shimadzu, Japan). The adsorption isotherms were evaluated for adsorbent surface area with the BET (Brunauer-Emmet-Teller) model by the instrument software (StarDriver v2.03). The soil extracts used for the incubation experiments were prepared as previously described (Pastore et al., 2020). Briefly, 100 g of each soil sample was placed in a polyethylene (PE) bottle, mixed with 1 l of distilled water and shaken at room temperature for 2 h using an overhead shaker. The extracts were filtered through cellulose filters with a particle retention range of 5–8 μm and pores such as to enable the passage of soil microorganisms and small particles of organic matter.

2.3. Chemical analyses of silicate parent material samples

In order to analyze the contents of total P (P_{tot}) and total Si (Si_{tot}) from the parent materials, crushed subsamples were digested using a combination of nitric acid (65% HNO_3), hydrofluoric acid (40% HF), and hydrochloric acid (37% HCl) according to Sandroni and Smith (2002) by ICP-OES (Vista-Pro radial, Varian). The specific absorption of radiation for Si and P was 253 nm and 190 nm, respectively. The reference material used for the analysis consisted of borosilicate glass (SiO_2 53.98%, LGC, SPS-SW2 surface water 2 for Si and SPS-WW2 waste water 2 for P).

2.4. Weathering of silicate parent materials

To determine the net Si and P solubilization rates from silicate parent

Table 1

Basic characteristics and description of the four forest soils and their parent materials at Bad Brückenau (BBR), Mitterfels (MIT), Vessertal (VES) and Conventwald (CON).

Site	Soil depth [cm]	C [g kg ⁻¹]	N [g kg ⁻¹]	P [g kg ⁻¹]	Microbial biomass C [mg kg ⁻¹]	Microbial biomass P [mg kg ⁻¹]	Specific surface area (SSA) of ground parent material [m ² g ⁻¹]	Total P of parent material [g kg ⁻¹]	Total Si of parent material [g kg ⁻¹]
BBR	30–35	42.0	3.2	2.5	170.4	2.0	16.7	3.05	190
	65–70	26.2	1.9	2.0	112.6	1.0	28.1	3.1	183
MIT	30–35	31.4	1.7	0.9	215.7	3.9	3.7	2.1	311
	65–70	26.8	1.4	0.9	140.8	3.3	5.7	1.8	278
VES	30–35	37.7	2.3	1.0	110.6	6.1	10.9	2.6	267
	65–70	12.8	0.8	0.9	102.9	7.8	10.9	2.7	263
CON	30–35	45.7	2.0	0.6	183.9	0.8	3.5	2.05	348
	65–70	7.7	0.6	0.4	126.6	1.2	6.1	0.6	274

Adapted from Lang et al., 2017.)

materials, three incubation experiments were conducted using soil extracts following Brucker et al. (2020) and Pastore et al. (2020). In experiment 1, the total Si and P mobilization rates from parent material were determined. For this purpose, 1 g of each parent material was incubated with 99 ml of the respective soil extract and 1 ml of glucose (3.33 mM). In addition, we performed a control experiment in analogy to experiment 1, but without addition of silicate parent material in order to quantify the mineralization of P from dissolved organic matter, which allowed us to correct the results of experiment 1 for P release from organic matter. Further, sterile control incubations were conducted to determine the effect of the soil extracts on Si and P solubilization. For this purpose, 99 ml of sterile soil solution and 1 ml of glucose (3.33 mM) were added to 1 g of each parent material. All experiments were performed in triplicate. Each incubation flask was loosely covered with aluminium foils which allowed the passage of air and continuously agitated at 20 °C for 14 days on a horizontal shaker.

2.5. Chemical analyses of soil extracts incubated with parent material

In each soil extract, dissolved Si was measured at 0, 7 and 14 days after the beginning of the experiment. Briefly, aliquots of 10 ml were taken and filtered through 0.45-µm cellulose acetate filters. The filtrates were acidified by adding 50 µl of 65% HNO₃ to prevent Si precipitation and then centrifuged at 1500×g for 15 min. The resulting supernatant was analysed for Si by ICP-OES (Vista-Pro radial, Varian, USA). In parallel, the amounts of phosphate released from the parent material in the soil extracts were also quantified. At defined time intervals (0, 2, 3, 5, 7, 11, and 14 days after the beginning of the experiment), 5 ml were taken from the flasks and vacuum filtered using 0.45 µm cellulose acetate filters. The resulting filtrates were analysed for pH and phosphate. The latter was determined according to the molybdenum-blue assay (Murphy and Riley, 1962) and measured with an Infinite M200 Pro microplate reader (Tecan, Switzerland).

2.6. Abundance of P-solubilizing bacteria

The relative abundance of P-solubilizing bacteria (PSB) was assessed by suspending 0.5 g of fresh soil in 49.5 ml of sterile water and shaking for 1 h. Serial dilutions (10⁻², 10⁻³) from each soil suspension were tested to identify the appropriate cell density. Subsequently, from each suspension, an aliquot of 100 µl was aseptically spread on Pikovskaya's agar medium (PVK) and the plates were incubated at 20 °C for 10 days. The PVK medium was composed of: 10 g glucose; 5 g hydroxyapatite; 0.5 g yeast extract; 0.5 g ammonium sulphate; 0.2 g potassium chloride; 0.2 g sodium chloride; 0.1 g magnesium sulphate; 0.002 g ferrous

sulphate; 0.002 g manganese sulphate and 15 g agar-agar in 1 l of distilled water (Pikovskaya, 1948). The pH of the solution was adjusted to 7.0. One-hundred colony-forming units (CFUs) from each soil sample were screened. If a bacterial colony dissolves hydroxyapatite, a halo (clear zone) becomes visible in the otherwise milky medium. In this case, the colony was considered to be formed by a PSB. The relative abundance of PSB was calculated by dividing the number of colonies formed by PSB by the total number of colonies and multiplying by 100.

2.7. Amplification and sequencing analysis of P-solubilizing bacteria (16S rRNA gene)

Bacterial colonies identified as PSB were collected from the PVK agar plates using sterile toothpicks and aseptically transferred into buffer solutions for DNA extraction. Detailed procedure describing amplification of 16S rRNA genes, quality trimming and annotation was provided previously by Widdig et al. (2019). Briefly, genomic DNA of bacterial colonies was extracted using the NucleoMag® Tissue kit on a KingFisher platform (Thermo Fisher Scientific, Massachusetts, USA) and diluted 100-fold with nuclease free water according to the manufacturer's instructions. The 16S fragment covering variable regions V5-V8 were amplified using primers 799F and 1391R as recommended in Beckers et al. (2016). PCR products were purified using the NucleoMag® 96 PCR cleanup kit. PCR products were sequenced (Sanger sequencing, GATC Biotech) using primer 799F.

2.8. Sequencing data analysis

Sequence data were processed using Geneious v. 11 (Biomatters Ltd., New Zealand). The sequences were searched for PCR primer sequences (799F and 1391R) and for low quality bases, which were excluded from sequence database searches. Sequence similarity searches were conducted against the nr/nt nucleotide database at NCBI as well as the NCBI RefSeq Loci 16S database. Sequences were aligned using MAFFT software (v. 7.388; Katoh and Standley, 2013). Sequences with a 98% cut-off similarity were clustered into operational taxonomic units (OTUs) and the name of the lowest common rank in the nomenclatural hierarchy was chosen. The OTU classification method is a commonly used approach to estimate microbial diversity and demonstrated to be ecologically consistent across habitats (Schmidt et al., 2014; Mysara et al., 2017). Only the non-redundant top hits were selected for taxonomic annotation. For this purpose, each sequence was compared with all other sequences and sequences sharing identity above 98% identity were assigned to one taxon. OTUs assignment was done using the NCBI database, considering that eleven species of the genus *Burkholderia* have

been transferred to the genus *Paraburkholderia* and three species of the genera *Burkholderia* have been transferred to the new genus *Caballeronia* gen. nov. which represents a distinctive clade in phylogenetic trees (Dobritsa and Samadpour, 2016). Major phylogenetic changes were detected at the order and genus levels. Based on their partial 16S rRNA gene sequence, a phylogenetic tree for each of the two most abundant genera (*Burkholderia* sp. and *Peanibacillus* sp.) was constructed, using *Ralstonia pickettii* (AY741342) and *Brevibacillus brevis* (AB271756) as outgroups, respectively. Phylogenetic trees were reconstructed and edited in MEGAX (v. 10.1.5) based on the neighbor-joining method with 1000 bootstrap replicates. The maximum composite likelihood method was the chosen distance method. The partial 16S rRNA gene sequences were deposited in GenBank (<https://www.ncbi.nlm.nih.gov/genbank/>) under the accession numbers MN727301-MN727311 and MN728272-MN728288.

2.9. Soil microbial biomass

Soil microbial biomass C (MBC) and P (MBP) were determined using the chloroform fumigation-extraction method (Brookes et al., 1982; Vance et al., 1987). Briefly, 10 g of fresh soil were split into two equal parts, of which 5 g were fumigated at room temperature for 24 h with ethanol-free CHCl_3 . Organic C was extracted from the fumigated and non-fumigated samples using 0.5 M K_2SO_4 with a soil: solution ratio of 1:5 and measured by a TOC/TN analyzer (Multi N/C 2100S, Analytik Jena, Germany). Dissolved P was extracted from the fumigated and non-fumigated samples using a solution of 0.025 M HCl and 0.03 M NH_4F (Bray-1 extractant) with a 1:10 soil to solution ratio (Bray and Kurtz, 1945) and determined using the molybdenum-blue assay (Murphy and Riley, 1962). Microbial biomass C and P were calculated as the difference between extractable C and P in the fumigated and non-fumigated soil samples using a conversion factor of 2.22 for MBC (Joergensen et al., 1996) and 2.5 for MBP (Brookes et al., 1982; Jen-

$$\text{Gross P solubilization rate (nmol d}^{-1}\text{)} = \frac{(\text{Net Si solubilization rate [nmol d}^{-1}\text{]} * \text{P content [g kg}^{-1}\text{]})}{\text{Si content [g kg}^{-1}\text{]}} \quad (3)$$

kinson et al., 2004).

2.10. Organic acids

The amounts of four organic acids (citric, oxalic, 2-keto-D-gluconic and D-gluconic) were determined in filtered samples from the soil extracts on day 7 and 14 after the beginning of the experiment. All filtrates were examined by means of high-performance liquid chromatography (Agilent series 1100, USA) coupled to a diode array HPLC detector (DAD) and a mass spectrometry (Agilent 6130 single quadrupole). Separation of the organic acids was carried out on a hydro-reversed-phase column (Phenomenex Synergi 4 u Hydro-RP 80A) combined with a guard column. Organic acids were identified based on their retention times and selected ions in negative ionization mode. Quantification was performed according to the external standard calibration method. HPLC-MS data were processed using the Agilent's Chemstation software package (v. 3.3.1). The amounts of each organic acid were calculated by multiplying the corresponding concentration (mg l^{-1}) in the soil extracts by the volume (l) present in the flask at the time of sampling and subsequently expressed in μmol . In addition, the concentration of the carboxylic groups was calculated from the concentrations of organic acids and the respective number of carboxyl groups they contain.

2.11. Calculation and statistics

The amounts of Si and P in the incubated soil extracts were calculated by multiplying the element concentration (nmol l^{-1}) by the volume (l) of the soil extract at the time of sampling. The total Si mobilization rates were computed according to the following equation (Eq. (1)):

$$\text{Total Si mobilization rate (nmol d}^{-1}\text{)} = \frac{(\text{Si[nmol]}_{\text{day14}} - \text{Si[nmol]}_{\text{day0}})}{14 [\text{days}]} \quad (1)$$

Where Si[nmol] represents the amount of Si at the end (day 14) and the beginning (day 0) of the experiment. Additionally, to determine the chemical effects of the soil extracts on the amounts of Si released from the silicate parent material, the amounts of Si released in the sterile control were also calculated. The net Si solubilization rate (nmol d^{-1} , Eq. (2)) from each silicate parent material was estimated as the difference between the total Si mobilization rate and the release rate determined in the sterile experiment:

$$\text{Net Si solubilization rate (nmol d}^{-1}\text{)} = \text{total Si mobilization rate (nmol d}^{-1}\text{)} - \text{Si release rate in sterile control (nmol d}^{-1}\text{)} \quad (2)$$

We consider this a net rate since we cannot exclude microbial immobilization (i.e., uptake) of Si. The net Si solubilization rates were divided by the corresponding amount of silicate parent material utilized as well as by the respective specific surface area ($\text{m}^2 \text{g}^{-1}$) of the ground parent material to result in a final rate expressed as $\text{nmol m}^{-2} \text{d}^{-1}$. Also, we estimated the solubilization of P from silicate parent materials based on the Si and P content of the parent materials and the Si solubilization rates using the equation below (Eq. (3)):

We consider this a gross rate because microbial immobilization (i.e., uptake) of P is not taken into account here and the net P solubilization is likely smaller due to microbial P immobilization. The gross P solubilization rates were divided by the corresponding amount of silicate parent material utilized as well as by the respective surface area ($\text{m}^2 \text{g}^{-1}$) to result in a final rate expressed as $\text{nmol m}^{-2} \text{d}^{-1}$. To check if variables were normally distributed, the Shapiro-Wilk test was performed ($P > 0.05$). Further, all data sets were tested for equality of variance using Levene's test. When variances were not significantly different between groups, analysis of variance (one-way ANOVA) was applied to test for differences between soil chemical properties, net Si solubilization rates and gross P solubilization rates. Differences in net Si solubilization rates and the relative abundance of PSB between the two soil depths of each soil were analysed by *t*-test followed by post-hoc Tukey HSD ($P < 0.05$). The non-parametric Kruskal-Wallis H test was used with a pairwise Wilcoxon test when variances were unequal. Relations between net Si solubilization rates and chemical properties of the soil extracts were assessed by Spearman rank correlations. Additionally, linear regressions for net Si solubilization and the variables pH and carboxyl groups ($-\text{COOH}$) determined in the soil extracts were conducted. All statistical analysis was performed using SigmaPlot (version 13.0, Systat Software, San Jose, California, USA).

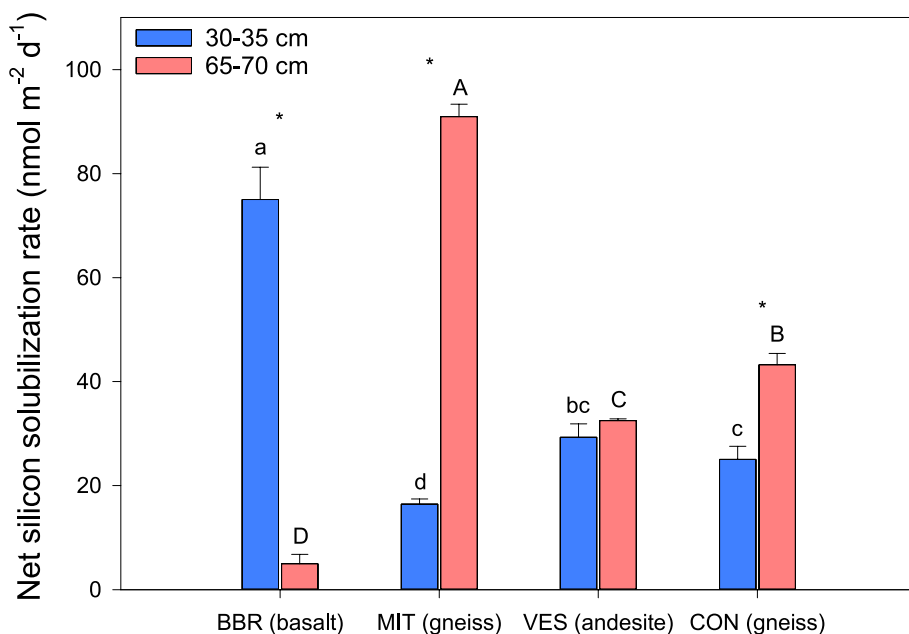


Fig. 1. Net Si solubilization rates for silicate parent materials incubated with glucose in aqueous extracts obtained from the four forest soils. The rates were calculated per specific surface area and over 14 days of incubation. The samples were taken at two soil depths (30–35 and 65–70 cm). Bars show means, and error bars indicate standard deviations ($n = 3$). Different letters indicate significant differences tested separately for the two soil depths by one-way ANOVA followed by post-hoc Tukey HDS ($P < 0.05$). Stars indicate significant differences between the two depths of each soil, tested by t -test followed by post-hoc Tukey HDS ($P < 0.05$).

3. Results

3.1. Net Si solubilization from silicate parent material

The concentrations of dissolved Si ranged between 2.9 and 13.0 mg l⁻¹ after two weeks of incubation of the soil with weathered parent materials and glucose. The concentrations of dissolved Si from weathered parent materials and autoclaved soil solution (sterile control) were equal on average to 0.4 mg l⁻¹. The Si concentrations were up to 32 times higher in the biotic experiment compared to the abiotic experiment, indicating that microbes strongly enhance silicate dissolution. Rates of Si solubilization normalized to the surface area of silicates differed significantly among the four soils and the two soil depth increments (Fig. 1). The net Si solubilization rate from the soil extracts incubated with the respective parent material and glucose ranged between 5.0 (± 1.8) and 91.0 (± 2.4) nmol m⁻² d⁻¹. At 30–35 cm depth, BBR (basalt) had the highest net Si solubilization rate in comparison to the other three sites, whereas MIT (paragneiss) had the lowest ($P < 0.05$). At 65–70 cm depth, the net Si solubilization rate in MIT was significantly higher than in the other soils (+70%; $P < 0.01$). We found that the Si concentrations increased during the first week of incubation, while the pH showed a twofold trend: it increased in the first 3 days and then decreased from day 4 to day 6 (Fig. S1). After day 7 no substantial changes in pH were recorded at all sites. At site MIT, the soil extracts from 65 to 70 cm depths showed the highest pH decline compared to the extracts from the other soils (Figs. S1–b). Further, linear regression analysis pointed out that the Si content of the parent material at 30–35 cm depth was negatively related with the Si solubilization rate ($R^2 = 0.63$, $P < 0.001$), whereas at 65–70 cm depth, a positive relationship was observed ($R^2 = 0.93$, $P < 0.001$).

3.2. P solubilization from silicate parent material

We did not measure net P solubilization but rather P immobilization, as indicated by a steady decline in the concentration of phosphate over the two-week period (data not shown). The likely reason for this is that microorganisms took up more P than they released from the parent material. However, we determined the gross P solubilization rates from the P and Si content of the parent materials and the Si solubilization rate based on stoichiometric considerations. This approach allowed us to estimate the gross release of P. Gross P solubilization ranged from 0.1

Table 2

P solubilization from four weathered parent materials at two different soil depths (30–35 and 60–65 cm). The stoichiometrically-derived gross P solubilization rates were determined according to the measured Si and P content of the respective weathered parent material and the amount of Si that was released over the course of 14 days. Mean values and standard deviations (\pm SD, in parentheses) are shown ($n = 3$). Uppercase and lowercase letters show significant differences tested separately for the two soil depths by one-way ANOVA, followed by post-hoc Tukey HDS ($P < 0.05$).

Site	Parent material	Soil depth [cm]	Gross P solubilization rate [nmol m ⁻² d ⁻¹] ^a
BBR	Basalt	30–35	1.1 (± 0.1) ^a
		65–70	0.1 (± 0.03) ^B
MIT	Paragneiss	30–35	0.1 (± 0.01) ^d
		65–70	0.5 (± 0.01) ^A
VES	Trachyandesite	30–35	0.3 (± 0.02) ^b
		65–70	0.3 (± 0.07) ^A
CON	Paragneiss	30–35	0.1 (± 0.01) ^c
		65–70	0.1 (± 0.00) ^B

^a Computed per g of parent material.

nmol m⁻² d⁻¹ (± 0.00) to 1.1 nmol m⁻² d⁻¹ (± 0.1). Overall, the gross P solubilization rates were significantly higher at the P-rich site (BBR) compared to the P-poor site (CON) in the upper soil depth (Table 2).

3.3. Organic acids in soil extracts

We found that the amounts of organic acids from BBR and VES were significantly larger than those measured at sites MIT and CON ($P < 0.05$). Further, our data show that monocarboxylic acids (D-gluconic and 2-keto-D-gluconic acid) represented together up to 88% of all detected acids. At site BBR, 2-keto-D-gluconic acid was found in higher amounts, whereas in the other three soil extracts D-gluconic acid was predominant (Fig. 2). We found that the sum of the four organic acids decreased significantly from day 7 to day 14 in all soil extracts (Fig. 2, P

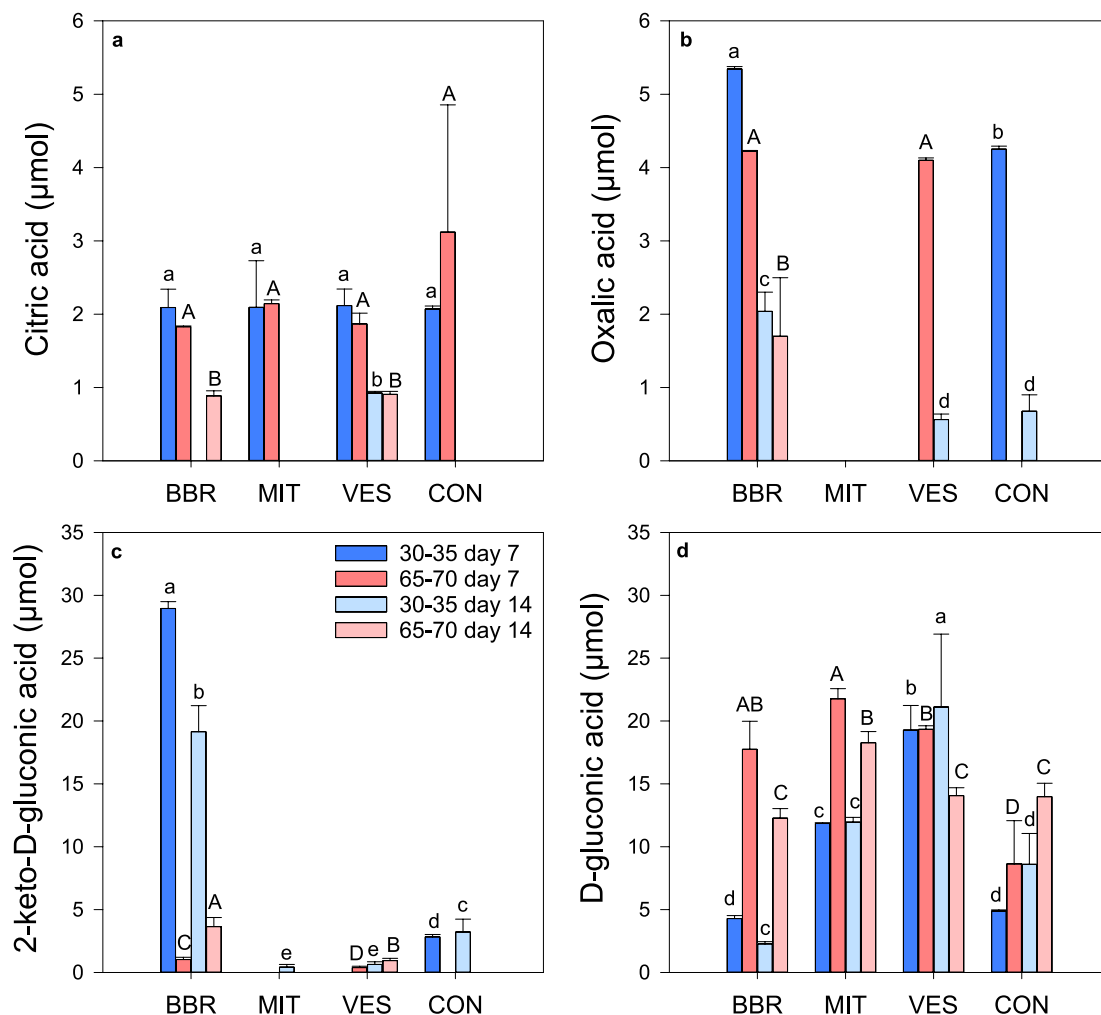


Fig. 2. Amounts of citric (a), oxalic (b), 2-keto-D-gluconic (c), and D-gluconic (d) acids measured at day 7 and 14 of the incubation experiment conducted with soil extracts from two different soil depths (30–35 and 65–70 cm). Bars represent means and error bars indicate standard deviations ($n = 3$). Different lowercase and uppercase letters show significant differences between soils and soil depths tested separately for day 7 and day 14 by one-way ANOVA followed by post-hoc Tukey HSD ($P < 0.05$). Stars indicate significant differences between two depths of one soil, tested by t -test followed by post-hoc Tukey HSD ($P < 0.05$).

Table 3

Relationships between the net Si solubilization rates (Si_{sol}) and the changes in pH (ΔpH) and the mean concentrations of carboxyl groups ($-\text{COOH}$) determined in the soil extracts over 14 days and calculated separately for the two soil depths (30–35 cm and 65–70 cm).

Mineral soil depth [cm]	Linear equation	Coefficient of determination (R^2) and p-value
30–35	$\text{Si}_{\text{sol}} = -3.0792x + (16.209 * \Delta\text{pH})$	0.43, $P < 0.05$
30–35	$\text{Si}_{\text{sol}} = 0.5979x - (3.1603 * \text{COOH})$	0.51, $P < 0.05$
65–70	$\text{Si}_{\text{sol}} = -5.7113x + (34.086 * \Delta\text{pH})$	0.73, $P < 0.05$
65–70	$\text{Si}_{\text{sol}} = 0.3093x + (4.7554 * \text{COOH})$	0.14, $P < 0.05$

< 0.05), except at site CON. Citric acid was detected only during the first week of incubation in MIT and CON, but not thereafter (Fig. 2-a). The amounts of carboxyl groups in the soil extracts were not significantly correlated with pH ($P > 0.05$). Also, we found that the amounts of carboxyl groups measured in the soil extracts at 30–35 cm depth explained 51% of the variation in the net Si solubilization, while at 65–70 cm depth they explained only 14% of the overall variability (Table 3).

3.4. Relative abundance and community composition of PSB

The relative abundance of PSB ranged from 2.0% to 22.1% of all bacterial colonies from all soils and soil depth increments (Fig. 3). Overall, we found that the relative abundance of PSB was significantly higher in CON (at both soil depths) than in any other soil ($P < 0.001$). At 65–70 cm depth, the abundance of PSB was significantly larger at site BBR than at MIT and VES. In total, 333 PSB colonies were identified by 16S rRNA gene sequence analysis. The sequenced PSB belonged to five phyla (Proteobacteria, Cyanobacteria, Firmicutes, Actinobacteria, Deinococcus–Thermus) and seven different classes (α -Proteobacteria,

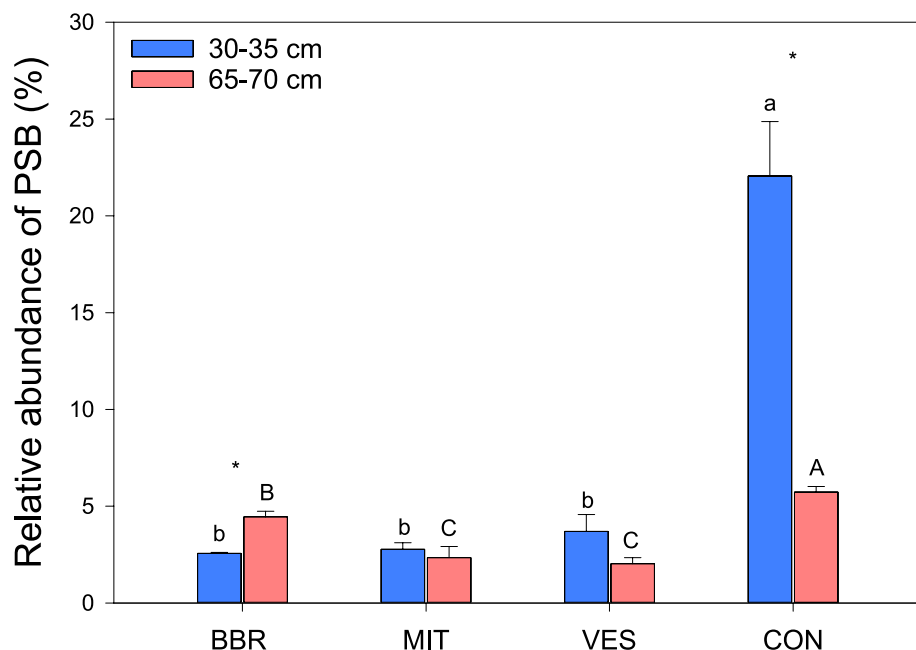


Fig. 3. Relative abundance of P-solubilizing bacteria (PSB) in the four forest soils at two different depths (30–35 and 65–70 cm). Bars represent means and error bars indicate standard deviations (n = 3). Different uppercase and lowercase letters indicate significant differences between sites tested separately for each soil depth using one-way ANOVA followed by post-hoc Tukey HSD (p < 0.05). Stars indicate significant differences between the two depths of each soil, tested by t-test followed by post-hoc Tukey HSD (P < 0.05).

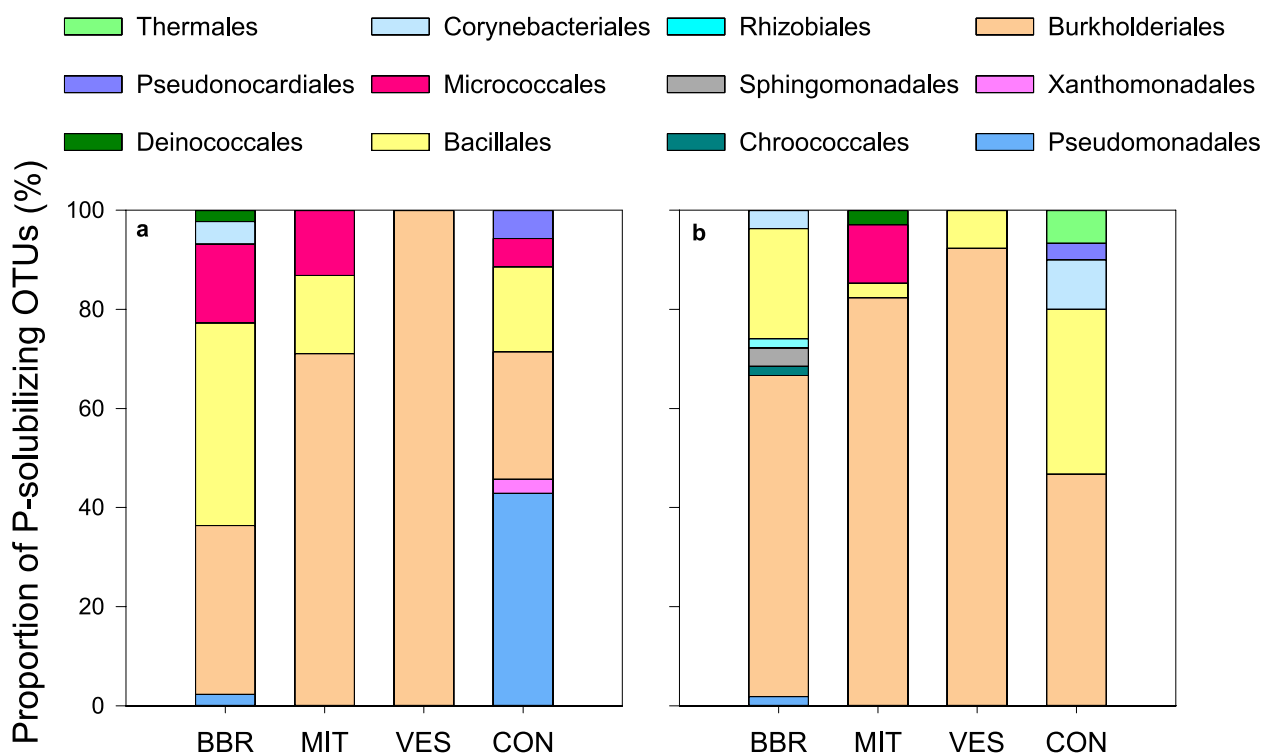


Fig. 4. Relative abundance of different OTUs of P-solubilizing bacteria (PSB) from four forest soils in 30–35 cm (a) and 60–65 cm (b) soil depth. Isolates identified as PSB were grouped into operational taxonomic units (OTU) at 98% cut-off similarity. Taxonomic classification of isolates is shown at the order level.

β -Proteobacteria, γ -Proteobacteria, Cyanophyceae, Bacilli, Actinobacteria, Deinococci). At 30–35 cm depth, *Bacillales* dominated at the site BBR and *Pseudomonadales* at site CON. *Burkholderiales* was the dominant order in MIT and VES (Fig. 4-a). At 65–70 cm depth, *Burkholderiales* were found to be the dominant order at all sites (Fig. 4-b). For comparative purposes with other studies, the relative abundance of

different OTUs of PSB is shown also at the genus level in the supplementary material (Fig. S2). We found that *Caballeronia* sp., *Collimonas* sp., *Paraburkholderia* sp. and *Paenibacillus* sp. were present in all soils, while *Herbaspirillum* sp. and *Variovorax* sp. were found in all soils except MIT and CON, respectively. Among all sequenced PSB colonies, 51 different OTUs were obtained as defined by clustering of the 16S rRNA

gene similarity. Of these, *Paenibacillus* (17 OTUs), *Burkholderia* (11 OTUs), and *Pseudomonas* (6 OTUs) were the most abundant across all sites. Since *Paenibacillus* sp. and *Burkholderia* sp. made up together at least 70% of all P-solubilizing OTUs across all sites, we further explored the species composition for the two genera. A significant genetic diversity existed within the same OTU species from the four tested soils. Overall, at site BBR we found the highest genetic diversity, while the lowest was found at site VES. The mineral composition of the bedrock had a strong effect on the distribution of *Burkholderia* species, but not on the distribution of *Paenibacillus* species (Figs. S3–S4).

4. Discussion

4.1. Factors controlling the weathering of silicate parent materials

Here we found that the Si solubilization rates were 7–32 times higher in the biotic experiment compared to the abiotic experiment (sterile conditions) indicating that microbes exert a strong biological control over the dissolution of silicates, especially when provided with an easily accessible C source. High Si concentrations in the solution went along with high P concentrations. The reason for this can be that Si and P compete for binding sites on mineral surfaces, as suggested by other authors who showed that with high concentrations of Si more P was dissolved in peat and permafrost soils (Schaller et al., 2019; Hömberg et al., 2020). We found a significant positive relationship between the carboxyl groups of the organic acids and the net Si solubilization rates (Table 3), in accordance with Hömberg et al. (2020). Organic acids accounted for 51% of the total variability in the net Si solubilization rates in the extracts from the upper soil depth. These findings suggest that organic acids effectively complexed metal cations present in the crystal lattice (i.e. Al, Fe, Ca, Mg) or served as silicon substituents (ligand exchange), thereby promoting the solubilization reaction (Liu et al., 2006; Violante et al., 2010; Smits and Wallander, 2017; Lee et al., 2019). Our results are in agreement with several previous studies reporting that the formation of stable complexes of metal ions and organic ligands results in an increase in dissolved Si in the soil solution (Welch and Ullman, 1993; Vandevivere et al., 1994; Blume et al., 2016). Dissolution rates depend on the amounts of functional groups (-COOH) that can react with mineral surfaces as well as on the strength of the bond that is established between the ligand (mono-, di- and tri-carboxylic acids) and the metal ion. The net Si solubilization rates from basalt (BBR) were up to three times higher than the net Si solubilization rates from paragneiss and andesite in the soil extracts from the upper soil depth (Fig. 1). As shown in Table S1, we found that the amounts of carboxyl groups at site BBR were 1.6–3.7 times higher than the amounts of carboxyl groups in the other soil extracts after seven days of incubation. Oxalic and 2-keto-D-gluconic acids made up together 84% of the total carboxyl groups measured in the soil extract from BBR (Fig. 2). Therefore, the higher dissolution of basalt compared to the other parent materials likely resulted from the higher amounts of carboxyl functional groups released by microbes in the soil BBR, especially mono- and di-carboxylic acids (Goldstein, 1995).

In the soil extracts from the lower soil depth, organic acids explained only 14% of the variation in the net Si solubilization rates, whereas the change in pH accounted for 73% of the total variability. Thus, in the lower soil depth, complexation by organic acids played only a marginal role for the Si solubilization rates possibly as a result of a lower soil microbial activity, as also described previously (Vandevivere et al., 1994; Sverdrup, 2009). The negative relationship between the decrease in pH (Δ pH) and the net Si solubilization rates suggests that the release of Si from silicates resulted from acidification of the soil extract. Our results agree with Drever (1994) who found that silicate dissolution rate

depends on pH: below pH 4–5, the rate increases with decreasing pH, in the circumneutral region the rate is pH-independent, and at pH values above 8 the rate increases with increasing pH. The decrease in pH (Δ pH) was particularly pronounced in the soil extracts from MIT and CON (paragneiss) where the pH significantly decreased during the incubation in comparison to the pH of the soil extracts from BBR (basalt) and VES (andesite). With decreasing pH of the soil extract there was an increase in the number of protons capable to binding to oxygen atoms at the mineral surfaces. Protonation induced increase in reactivity of surface sites weakens the metal cations-oxygen bonds, thus favoring dissolution of the mineral (Hinsinger, 2001; Brown et al., 2008). Taken together our findings confirm the first hypothesis that the dissolution of silicates in these acid soil extracts is primarily controlled by a decrease in pH and the release of organic acids by microbes (Harley and Gilkes, 2000; Cama and Ganor, 2006). In addition, this study shows how the general mechanisms of silicates dissolution are impacted by the different organic acids released by microbes from different soils and soil depths.

4.2. Organic acids

We found that the amounts of organic acids released by microbial communities in our study were fairly low compared to other solubilization experiments (Frey et al., 2010; Li et al., 2016) which we relate to the initial acidic conditions of our soil extracts. Marra et al. (2015) showed that the pH of the soil solution significantly affects the growth as well as the biochemical processes that microbes perform and, therefore, the total amounts of acids they produce. Marra et al. (2015) showed that at a relatively high pH (~pH 7.0), the production of organic acids was up to 25% greater than at pH 5.0, which was the mean pH measured in our experiments. The organic acid concentrations decreased over time indicating that microbes may have quickly faced conditions of low C availability. In addition, the increase in pH in the soil extracts during the first 3 days of incubation suggests the metabolization (decomposition) of organic acids by organisms at the early stages of the experiment (Jones et al., 2003; Sauer et al., 2008). Most of the pH variation in the soil extracts took place in the first days of incubation (Fig. S1). Therefore, it is plausible that the production of organic acids must have been high during this phase, in particular after glucose addition, to then decline thereafter. Therefore, the relatively low detection of organic acids at day seven of the incubation might be the result of previous intense microbial utilization of organic acids, similarly to what was documented by Menezes-Blackburn et al. (2016) who found that nearly all organic acids were degraded by soil microbes within 24 h of incubation.

Considering the pK_a values of the four tested organic acids, their total amounts as well as the pH values of the solutions, only 8.9%–10.1% of protons released during the incubations were likely derived from organic acids after 7 days of incubation, when the peak of solubilization occurred. Therefore, the production of organic acids by microbes did not contribute significantly to the acidification of the soil extracts from day 7 to day 14. We assume that the acidification of the soil extracts was mainly due to carbonic acid production based on CO_2 respired by the microorganisms (Cornelis and Delvaux, 2016; Kanakiya et al., 2017).

4.3. The role of parent material in P nutrition strategies

Our results suggest that the gross P solubilization rates from parent materials in the upper soil depth were ~11 times higher at the P-rich site (BBR) compared to the P-poor site (CON) (Table 2). This finding supports the idea that the proportion of plant-available P derived from the bedrock, as opposed to that derived from the soil organic matter, decreases along the geosequence of the four soils from BBR to CON (Lang et al., 2017). As hypothesized by Lang et al. (2016), plant and microbes

at sites rich in mineral-bound P introduce P from primary minerals into the P cycle (acquiring systems). In contrast, ecosystems poor in mineral-bound P recycle P between soils and plants more efficiently (recycling systems). Overall, the gross P solubilization rates calculated for basalt (BBR) and andesite (VES) point out at a higher release of P from these weathered rocks than for paragneiss (MIT, CON) (Table 2). Similarly, some authors indicated that basalts have a larger weathering rate than other major continental silicate rocks (Dessert et al., 2003; Wolff-Boenisch et al., 2006). Taken together, our findings partially confirm the second hypothesis that in the upper soil depth, the rates of microbial gross P solubilization increased with decreasing crystallinity of the weathered bedrock (paragneiss < andesite < basalt).

4.4. Abundance and activity of PSB

We found that the abundance of PSB in the four mineral soils ranged from 2% at VES to 22.1% at CON (Fig. 3) which is in accordance with previous studies reporting that the relative abundance of PSB ranges from 0.5% to 53% in soils (Kucey, 1983; Chen et al., 2006; Browne et al., 2009; Azziz et al., 2012; Widdig et al., 2019). The higher relative abundance of PSB in P-poor environments such as CON might be the result of a selective pressure which favors organisms that actively mobilize inorganic P when P is scarce. The lower occurrence of PSB in nutrient-rich soils might be related to a lower microbial investment in the processes of P solubilization when nutrients are easily available. This finding is in accordance with other authors who found that the abundance of PSB is higher in P-poor environments than in P-rich environments (Mander et al., 2012; Nicolitch et al., 2016; Widdig et al., 2019; Spohn et al., 2020). The higher abundance of PSB at the P-poor site (CON) fits well with the high P release rates from hydroxyapatite at this site (Pastore et al., 2020), indicating that the abundance of PSB is related to the capacity of the microbial community to release P from apatite. On the contrary, despite the higher abundance of PSB at the P-poor site (CON) the gross P solubilization rates from the parent material at this site (paragneiss) were relatively low. This apparent incongruence was likely due to the fact that all structurally complex silicates undergo a stepwise weathering in the natural environment and that apatites are shielded by other minerals from biochemical weathering (White, 2003).

4.5. Diversity of PSB communities

We found that *Burkholderiales* and *Bacillales* together were by far the two most abundant bacterial orders in all soils and depths (Fig. 4). Results from the BLASTn analysis showed a high intraspecific diversity within *Burkholderiales* and *Bacillales*, especially at sites BBR and CON. *Burkholderiales* and *Bacillales* are adapted to live in C and N-rich environments (Fierer et al., 2007; Mandic-Mulec et al., 2015). We observed that the distribution of *Burkholderiales* seems highly influenced by the mineral chemistry of the rocks, with some members enriched in the presence of high-weatherable minerals and others enriched in the presence of less-weatherable minerals. *Bacillales* appeared less affected by the mineral composition of the rocks, and thus showed no significant variations between the different parent materials (Fig. S4). This finding fits with the recent view that members within the same bacterial order might be adapted to different functional strategies (Ho et al., 2017). Notably, we found the genus *Arthrobacter* only at sites BBR and MIT. This finding is of particular interest since the studied soils are characterized by the prevalence of P bound to Fe oxyhydroxides (Prietz et al., 2016) and members of the genus *Arthrobacter* are relatively effective at mobilizing iron (Nicolitch et al., 2019). Our data show that the genus *Pseudomonas*, which is reputed to have superior P solubilization ability among the PSB (Gulati et al., 2008; Browne et al., 2009), was only found at the P-poor site CON, suggesting the existence of a selective advantage for bacteria with this functional trait under P-poor conditions. As detailed in Fig. S2, *Pseudomonas* predominated in the upper soil depth. Some authors (Sutra et al., 2000; Qessaoui et al., 2019) showed that

members of the genus *Pseudomonas* represent typically root-associated microorganisms and might have positive effects on plant yields.

Soil PSB are known to also solubilize Si (Kang et al., 2017; Adhikari et al., 2020). We found that the highest release of Si occurred at site BBR and coincided with a significant prevalence of *Bacillales* which represented alone 41% of all PSB OTUs in this soil. Olsson-Francis et al. (2015) found that *Bacillales* solubilized up to 32.8% more Si from basalt than other bacterial groups. Surprisingly, in the lower soil depth, the highest Si solubilization rates were measured at site MIT where *Burkholderiales* represented ~80% of all PSB OTUs. Previous studies showed that the members of the genus *Burkholderia* exhibit stronger mineral weathering effectiveness compared to members of the genera *Bacillus* and *Paenibacillus* (Collignon et al., 2011; Lepleux et al., 2012; Wang et al., 2014; Nicolitch et al., 2019). Therefore, the high release of Si from paragneiss at site MIT might be due to the higher occurrence of *Burkholderia alpina* that likely acidified the soil extract. Our findings are partially in accordance with Bist et al. (2020) who showed that *Bacillus* and *Pseudomonas* in addition to *Sphingobacterium* have the capacity to strongly solubilize Si.

5. Conclusions

Taken together, we found that Si solubilization was increased by microbial activity. Si solubilization was negatively related to the observed decrease in pH (proton-promoted dissolution) and positively related to organic acids released by microbes (ligand-promoted dissolution). The four measured organic acids did not contribute significantly to the acidification of the soil extracts. Thus, the acidification was likely due to carbonic acid production based on CO₂ respired by microorganisms. Stoichiometrically-derived gross P solubilization rates in the upper soil depth were much higher at the P-rich site (BBR) compared to the P-poor site (CON). However, at site CON we found a significantly higher abundance of PSB compared to other soils. This finding might be related to a higher microbial investment in the processes of P solubilization in the P-poor soil, suggesting that P availability is a selective force driving the occurrence of bacteria with this functional trait. Overall, *Burkholderiales* and *Bacillales* were the two most widely occurring PSB OTUs across the four mineral soils and the genus *Pseudomonas*, reputed to have superior P solubilization ability among the PSB, was only found at the P-poor site. In conclusion, this study shows that the activity and the taxonomic composition of PSB varied significantly across the four forest soils and underpinned the observed differences in Si solubilization rates.

Declaration of competing interest

The authors declare that they have no known competing financial interests or personal relationships that could have appeared to influence the work reported in this paper.

Acknowledgements

This research was funded by the German Research Foundation (DFG) as part of the project SP 1389/4-2 of the priority program "Ecosystem nutrition: Forest strategies for limited phosphorus resources". The authors gratefully acknowledge the assistance of Alfons Weig, Michaela Hochholzer and Andrea Kirpal of the Keylab for Genomics and Bioinformatics for sequencing the bacterial colonies. We thank Baoli Zhu and Dheeraj Kanaparthi for assistance with the phylogenetic trees. Further, we thank Eduardo Vazquez, Meike Widdig and Alexander Guhr for their helpful comments on a previous version of the manuscript. We also thank members of the Laboratory for Analytical Chemistry (BayCEER) for the chemical analyses. Further, we thank Karin Söllner, Renate Krauß and Ralf Mertel for assistance provided in the laboratory. Thanks to Uwe Hell for help in sample collection and handling of the silicate parent materials.

Appendix A. Supplementary data

Supplementary data to this article can be found online at <https://doi.org/10.1016/j.soilbio.2020.108050>.

References

- Achat, D.L., Bakker, M.R., Zeller, B., Pellerin, S., Bienaimé, S., Morel, C., 2010. Long-term organic phosphorus mineralization in spodosols under forests and its relation to carbon and nitrogen mineralization. *Soil Biology & Biochemistry* 42, 1479–1490. <https://doi.org/10.1016/j.soilbio.2010.05.020>.
- Adhikari, A., Lee, K.E., Khan, M.A., Kang, S.M., Adhikari, B., Imran, M., Jan, M., Kim, K. M., Lee, I.J., 2020. Effect of silicate and phosphate solubilizing rhizobacterium *Enterobacter ludwigii* GAK2 on *Oryza sativa* L. under cadmium stress. *Journal of Microbiology and Biotechnology* 30, 118–126. <https://doi.org/10.4014/jmb.1906.06010>.
- Ågren, G.I., Wetterstedt, J.Å.M., Billberger, M.F.K., 2012. Nutrient limitation on terrestrial plant growth – modeling the interaction between nitrogen and phosphorus. *New Phytologist* 194, 953–960. <https://doi.org/10.1111/j.1469-8137.2012.04116.x>.
- Azziz, G., Bajsa, N., Haghjoui, T., Taulé, C., Valverde, A., Igual, J., Arias, A., 2012. Abundance, diversity and prospecting of culturable phosphate solubilizing bacteria on soils under crop–pasture rotations in a no-tillage regime in Uruguay. *Applied Soil Ecology* 61, 320–326. <https://doi.org/10.1016/j.apsoil.2011.10.004>.
- Bacon, C.R., 1992. Partially melted granodiorite and related rocks ejected from crater lake caldera, Oregon. In: Brown, Chappell (Eds.), *The Second Hutton Symposium on the Origin of Granites and Related Rocks*, 83. Transactions of the Royal Society of Edinburgh: Earth Sciences, pp. 27–47. <https://doi.org/10.1017/S0263593300007732>.
- Banfield, J.F., Barker, W.W., Welch, S.A., Taunton, A., 1999. Biological impact on mineral dissolution: application of the lichen model to understanding mineral weathering in the rhizosphere. *Proceedings of the National Academy of Sciences of the United States of America* 96, 3404–3411. <https://doi.org/10.1073/pnas.96.7.3404>.
- Beckers, B., Op De Beeck, M., Thijs, S., Truyens, S., Weyens, N., Boerjan, W., Vangronsveld, J., 2016. Performance of 16s rDNA primer pairs in the study of rhizosphere and endosphere bacterial microbiomes in metabarcoding studies. *Frontiers in Microbiology* 7, 650. <https://doi.org/10.3389/fmicb.2016.00650>.
- Bist, V., Niranjana, A., Ranjan, M., Lehri, A., Seem, K., Srivastava, S., 2020. Silicon-solubilizing media and its implication for characterization of bacteria to mitigate biotic stress. *Frontiers of Plant Science* 11, 28. <https://doi.org/10.3389/fpls.2020.00028>.
- Blume, H.P., Brümmer, G.W., Fleige, H., Horn, R., Kandeler, E., Kögel-Knabner, I., Kretzschmar, R., Stahr, K., Wilke, B.M., 2016. Inorganic soil components – minerals and rocks. In: Stahr, K. (Ed.), *Scheffer/Schachtschabel Soil Science*. Springer-Verlag GmbH Berlin Heidelberg, pp. 7–52. https://doi.org/10.1007/978-3-642-30942-7_2.
- Bray, R.H., Kurtz, L.T., 1945. Determination of total, organic, and available forms of phosphorus in soils. *Soil Science* 59, 39–45. <https://doi.org/10.1097/00010694-194501000-00006>.
- Brookes, P.C., Powlson, D.S., Jenkinson, D.S., 1982. Measurement of microbial biomass phosphorus in soil. *Soil Biology & Biochemistry* 14, 319–329. [https://doi.org/10.1016/0038-0717\(82\)90001-3](https://doi.org/10.1016/0038-0717(82)90001-3).
- Browne, P., Rice, O., Miller, S.H., Burke, J., Dowling, D.N., Morrissey, J.P., O’Gara, F., 2009. Superior inorganic phosphate solubilization is linked to phylogeny within the *Pseudomonas fluorescens* complex. *Applied Soil Ecology* 43, 131–138. <https://doi.org/10.1016/j.apsoil.2009.06.010>.
- Brucker, E., Sarmite, K., Spohn, M., 2020. Release of phosphorus and silicon from minerals by soil microorganisms depends on the availability of organic carbon. *Soil Biology & Biochemistry* 143, 107737. <https://doi.org/10.1016/j.soilbio.2020.107737>.
- Bünemann, E.K., 2015. Assessment of gross and net mineralization rates of soil organic phosphorus - a review. *Soil Biology and Biochemistry* 89, 82–98. <https://doi.org/10.1016/j.soilbio.2015.06.026>.
- Cama, J., Ganor, J., 2006. The effects of organic acids on the dissolution of silicate minerals: a case study of oxalate catalysis of kaolinite dissolution. *Geochimica et Cosmochimica Acta* 70, 2191–2209. <https://doi.org/10.1016/j.gca.2006.01.028>.
- Chen, Y.P., Rekha, P.D., Arun, A.B., Shen, F.T., Lai, W.-A., Young, C.C., 2006. Phosphate solubilizing bacteria from subtropical soil and their tricalcium phosphate solubilizing abilities. *Applied Soil Ecology* 34, 33–41. <https://doi.org/10.1016/j.apsoil.2005.12.002>.
- Chung, H., Park, M., Madhaiyan, M., Seshadri, S., Song, J., Cho, H., Sa, T., 2005. Isolation and characterization of phosphate solubilizing bacteria from the rhizosphere of crop plants of Korea. *Soil Biology & Biochemistry* 37, 1970–1974. <https://doi.org/10.1016/j.soilbio.2005.02.025>.
- Collignon, C., Uroz, S., Turpault, M., Frey-Klett, P., 2011. Seasons differently impact the structure of mineral weathering bacterial communities in beech and spruce stands. *Soil Biology & Biochemistry* 43, 2012. <https://doi.org/10.1016/j.soilbio.2011.05.008>, 2022.
- Cornelis, J.T., Delvaux, B., 2016. Soil processes drive the biological silicon feedback loop. *Functional Ecology* 30, 1298–1310. <https://doi.org/10.1111/1365-2435.12704>.
- Dessert, C., Dupré, B., Gaillardet, J., Francois, L.M., Allègre, C.J., 2003. Basalt weathering laws and the impact of basalt weathering on the global carbon cycle. *Chemical Geology* 202, 257–273. <https://doi.org/10.1016/j.chemgeo.2002.10.001>.
- Dobritsa, A.P., Samadpour, M., 2016. Transfer of eleven species of the genus *Burkholderia* to the genus *Paraburkholderia* and proposal of *Caballeronia* gen. nov. to accommodate twelve species of the genera *Burkholderia* and *Paraburkholderia*. *International Journal of Systematic and Evolutionary Microbiology* 66, 2836–2846. <https://doi.org/10.1099/ijsem.0.001065>.
- Duboc, O., Robbe, A., Santner, J., Folegnani, G., Gallais, P., Lecanuet, C., Zehetner, F., Nagl, P., Wenzel, W., 2019. Silicon availability from chemically diverse fertilizers and secondary raw materials. *Environmental Science and Technology* 53, 5359–5368. <https://doi.org/10.1021/acs.est.8b06597>.
- Drever, J.I., 1994. The effect of land plants on weathering rates of silicate minerals. *Geochimica et Cosmochimica Acta* 58, 2325–2332. [https://doi.org/10.1016/0016-7037\(94\)90013-2](https://doi.org/10.1016/0016-7037(94)90013-2).
- Fierer, N., Bradford, M.A., Jackson, R.B., 2007. Toward an ecological classification of soil bacteria. *Ecology* 88, 1354–1364. <https://doi.org/10.1890/05-1839>.
- Frey, B., Rieder, S.R., Brunner, I., Plötze, M., Koetzsch, S., Lapanje, A., Brandl, H., Furrer, G., 2010. Weathering-associated bacteria from the damma glacier forefield: physiological capabilities and impact on granite dissolution. *Applied and Environmental Microbiology* 76, 4788–4796. <https://doi.org/10.1128/AEM.00657-10>.
- Gleeson, B.D., Kennedy, N.M., Clipson, N., Melville, K., Gadd, G.M., McDermott, F.P., 2006. Characterization of bacterial community structure on a weathered pegmatitic granite. *Microbial Ecology* 51, 526–534. <https://doi.org/10.1007/s00248-006-9052-x>.
- Goldstein, A.H., 1995. Recent progress in understanding the molecular genetics and biochemistry of calcium phosphate solubilization by gram negative bacteria. *Biological Agriculture and Horticulture* 12, 185–193. <https://doi.org/10.1080/01448765.1995.9754736>.
- Guntzer, F., Keller, C., Meunier, J.D., 2012. Benefits of plant silicon for crops: a review, 32. *Agronomy for Sustainable Development*, pp. 201–213. <https://doi.org/10.1007/s13593-011-0039-8>.
- Gulati, A., Rahi, P., Vyas, P., 2008. Characterization of phosphate-solubilizing fluorescent pseudomonads from the rhizosphere of sea buckthorn growing in the cold deserts of Himalayas. *Current Microbiology* 56, 73–79. <https://doi.org/10.1007/s00284-007-9042-3>.
- Haynes, R.J., Zhou, Y.-F., 2020. Silicate sorption and desorption by a Si-deficient soil – effects of pH and period of contact. *Geoderma* 365, 114204. <https://doi.org/10.1016/j.geoderma.2020.114204>.
- Harley, A.D., Gilkes, R.J., 2000. Factors influencing the release of plant nutrient elements from silicate rock powders: a geochemical overview. *Nutrient Cycling in Agroecosystems* 56, 11–36. <https://doi.org/10.1023/A:1009859309453>.
- Hinsinger, P., 2001. Bioavailability of soil inorganic P in the rhizosphere as affected by root-induced chemical changes: a review. *Plant and Soil* 237, 173–195. <https://doi.org/10.1023/A:1013351617532>.
- Ho, A., Di Lonardo, D.P., Bodelier, P.L., 2017. Revisiting life strategy concepts in environmental microbial ecology. *FEMS Microbiology Ecology* 93, 1–14. <https://doi.org/10.1093/femsec/fix006>.
- Hömberg, A., Obst, M., Knorr, K.H., Kalbitz, K., Schaller, J., 2020. Increased silicon concentration in fen peat leads to a release of iron and phosphate and changes in the composition of dissolved organic matter. *Geoderma* 374, 114422. <https://doi.org/10.1016/j.geoderma.2020.114422>.
- Huang, P.M., Wang, M.K., 2005. Minerals, primary. *Encyclopedia of Soils in the Environment*, pp. 500–510. <https://doi.org/10.1016/B0-12-348530-4/00464-1>.
- Jenkinson, D.S., Brookes, P.C., Powlson, D.S., 2004. Measuring soil microbial biomass. *Soil Biology & Biochemistry* 36, 5–7. <https://doi.org/10.1016/j.soilbio.2003.10.002>.
- Jones, L.D., Dennis, P.G., Owen, A.G., Van Hees, P.A.W., 2003. Organic acids behavior in soils – misconceptions and knowledge gaps. *Plant and Soil* 248, 31–41. <https://doi.org/10.1023/A:1022304332313>.
- Kang, S.M., Waqas, M., Shahzad, R., You, Y.H., Asaf, S., Khan, M.A., Lee, K.E., Joo, G.J., Kim, S.J., Lee, I.J., 2017. Isolation and characterization of a novel silicate-solubilizing bacterial strain *Burkholderia eburnea* CS4-2 that promotes growth of japonica rice (*Oryza sativa* L. cv. Dongjin). *Soil Science and Plant Nutrition* 63, 233–241. <https://doi.org/10.1080/00380768.2017.1314829>.
- Kanakiya, S., Adam, L., Esteban, L., Rowe, M.C., Shane, P., 2017. Dissolution and secondary mineral precipitation in basalts due to reactions with carbonic acid. *Journal of Geophysical Research: Solid Earth* 122, 4312–4327. <https://doi.org/10.1002/2017JB014019>.
- Katoh, K., Standley, D.M., 2013. MAFFT multiple sequence alignment software version 7: improvements in performance and usability. *Molecular Biology and Evolution* 30, 772–780. <https://doi.org/10.1093/molbev/mst010>.
- Kpombrekou, K., Tabatabai, M.A., 1994. Effect of organic acids on release of phosphorus from phosphate rocks. *Soil Science* 158, 442–453. <https://doi.org/10.1097/00010694-199415860-00006>.
- Kucey, R.M.N., 1983. Phosphate-solubilizing bacteria and fungi in various cultivated and virgin Alberta soils. *Canadian Journal of Soil Science* 63, 671–678. <https://doi.org/10.4141/cjss83-068>.
- Lang, F., Bauhus, J., Frossard, E., George, E., Kaiser, K., Kaupenjohann, M., Krüger, J., Matzner, E., Polle, A., Prietzel, J., Rennenberg, H., Wellbrock, N., 2016. Phosphorus in forest ecosystems: new insights from an ecosystem nutrition perspective. *Journal of Plant Nutrition and Soil Science* 179, 129–135. <https://doi.org/10.1002/jpln.201500541>.
- Lang, F., Krüger, J., Amelung, W., Willbold, S., Frossard, E., Bünemann, E.K., Bauhus, J., Nitschke, N., Kandeler, E., Marhan, S., Schulz, S., Bergkemper, F., Schloter, M., Luster, J., Guggisberg, F., Kaiser, K., Mikutta, R., Guggenberger, G., Polle, A., Pena, R., Prietzel, J., Rodionov, A., Talkner, U., Meessenburg, H., von Wilpert, K., Hölscher, A., Dietrich, H.P., Chmara, I., 2017. Soil phosphorus supply controls P

- nutrition strategies of beech forest ecosystems in Central Europe. *Biogeochemistry* 136, 5–29. <https://doi.org/10.1007/s10533-017-0375-0>.
- Lee, K.E., Adhikari, A., Kang, S.M., You, Y.H., Joo, G.J., Kim, J.O., Kim, S.J., Lee, I.-J., 2019. Isolation and characterization of the high silicate and phosphate solubilizing novel strain *Enterobacter ludwigii* GAK2 that promotes growth in rice plants. *Agronomy* 9, 144. <https://doi.org/10.3390/agronomy9030144>.
- Lepleux, C., Turpault, M.P., Oger, P., Frey-Klett, P., Uroz, S., 2012. Correlation of the abundance of betaproteobacteria on mineral surfaces with mineral weathering in forest soils. *Applied and Environmental Microbiology* 78, 7114–7119. <https://doi.org/10.1128/AEM.00996-12>.
- Liang, Y., Nikolic, M., Belanger, R., Gong, G., Song, A., 2015. In: Liang, Y., Nikolic, M., Belanger, R., Gong, G., Song, A. (Eds.), *Silicon Biogeochemistry and Bioavailability in Soil*. Silicon in Agriculture. Springer, Dordrecht, the Netherlands, pp. 45–68.
- Li, Z., Bai, T., Dai, L., Wang, F., Tao, J., Meng, S., Hu, Y., Wang, S., Hu, S., 2016. A study of organic acid production in contrasts between two phosphate solubilizing fungi: *Penicillium oxalicum* and *Aspergillus niger*. *Scientific Reports* 6, 25313. <https://doi.org/10.1038/srep25313>.
- Lindsay, W.L., 1979. *Chemical Equilibria in Soils*. John Wiley and Sons, New York, pp. 1–449.
- Liu, W., Xu, X., Wu, X., Yang, Q., Luo, Y., Christie, P., 2006. Decomposition of silicate minerals by *Bacillus mucilaginosus* in liquid culture. *Environmental Geochemistry and Health* 28, 133–140. <https://doi.org/10.1007/s10653-005-9022-0>.
- Ma, J.F., 2004. Role of silicon in enhancing the resistance of plants to biotic and abiotic stresses. *Soil Science and Plant Nutrition* 50, 11–18. <https://doi.org/10.1080/00380768.2004.10408447>.
- Malhotra, H., Vandana, Sharma S., Pandey, R., 2018. Phosphorus nutrition: plant growth in response to deficiency and excess. In: Hasanuzzaman, M., Fujita, M., Oku, H., Nahar, K., Hawrylak-Nowak, B. (Eds.), *Plant Nutrients and Abiotic Stress Tolerance*. Springer, Singapore. https://doi.org/10.1007/978-981-10-9044-8_7.
- Mander, C., Wakelin, S., Young, S., Condon, L., O'Callaghan, M., 2012. Incidence and diversity of phosphate-solubilising bacteria are linked to phosphorus status in grassland soils. *Soil Biology & Biochemistry* 44, 93–101. <https://doi.org/10.1016/j.soilbio.2011.09.009>.
- Mandic-Mulec, I., Stefanic, P., van Elsland, J.D., 2015. Ecology of *bacillaceae*. *Microbiology Spectrum* 3, 1–24. <https://doi.org/10.1128/microbiolspec.TBS-0017-2013>.
- Marra, L.M., de Oliveira-Longatti, S.M., Soares, C.R., de Lima, J.M., Olivares, F.L., Moreira, F.M., 2015. Initial pH of medium affects organic acids production but do not affect phosphate solubilization. *Brazilian Journal of Microbiology* 46, 367–375. <https://doi.org/10.1590/S1517-838246246220131102>.
- Mehmood, A., Akhtar, M., Imran Baloch, M., Rukh, S., 2018. Soil apatite loss rate across different parent materials. *Geoderma* 310, 218–229. <https://doi.org/10.1016/j.geoderma.2017.09.036>.
- Menezes-Blackburn, D., Paredes, C., Zhang, H., Giles, C.D., Darch, T., Stutter, M., George, T.S., Shand, C., Lumsdon, D., Cooper, P., Wendler, R., Brown, L., Blackwell, M., Wearing, C., Haygarth, P.M., 2016. Organic acids regulation of chemical-microbial phosphorus transformations in soils. *Environmental Science and Technology* 50, 11521–11531. <https://doi.org/10.1021/acs.est.6b03017>.
- Mysara, M., Vandamme, P., Props, R., Kerckhof, F.M., Leys, N., Boon, N., Raes, J., Monsieurs, P., 2017. Reconciliation between operational taxonomic units and species boundaries. *FEMS Microbiology Ecology* 93, fix029.
- Murphy, J., Riley, J.P., 1962. A modified single solution method for the determination of phosphate in natural waters. *Analytica Chimica Acta* 26, 678–681. [https://doi.org/10.1016/S0003-2670\(00\)88444-5](https://doi.org/10.1016/S0003-2670(00)88444-5).
- Nezat, C., Blum, J., Yanai, R., Hamburg, S., 2007. A sequential extraction to determine the distribution of apatite in granitoid soil mineral pools with application to weathering at the Hubbard Brook Experimental Forest, NH, USA. *Applied Geochemistry* 22, 2406–2421. <https://doi.org/10.1016/j.apgeochem.2007.06.012>.
- Nicolitch, O., Colin, Y.M., Turpault, P., Uroz, S., 2016. Soil type determines the distribution of nutrient mobilizing bacterial communities in the rhizosphere of beech trees. *Soil Biology & Biochemistry* 103, 429–445. <https://doi.org/10.1016/j.soilbio.2016.09.018>.
- Nicolitch, O., Feucherolles, M., Churin, J., Fauchery, L., Turpault, M.P., Uroz, S., 2019. A microcosm approach highlights the response of soil mineral weathering bacterial communities to an increase of K and Mg availability. *Scientific Reports* 9, 14403. <https://doi.org/10.1038/s41598-019-50730-y>.
- Oburger, E., Jones, D.L., Wenzel, W.W., 2011. Phosphorus saturation and pH differentially regulate the efficiency of organic acid anion-mediated P solubilization mechanisms in soil. *Plant and Soil* 341, 363–382. <https://doi.org/10.1007/s11104-010-0650-5>.
- Olsson-Francis, K., Boardman, C., Pearson, V., Schofield, P., Oliver, A., Summers, S., 2015. A culture-independent and culture-dependent study of the bacterial community from the bedrock soil interface. *Advances in Microbiology* 5, 842–857. <https://doi.org/10.4236/aim.2015.513089>.
- Oteino, N., Lally, R.D., Kivanuka, S., Lloyd, A., Ryan, D., Germaine, K.J., Dowling, D.N., 2015. Plant growth promotion induced by phosphate solubilizing endophytic *Pseudomonas* isolates. *Frontiers in Microbiology* 6, 745. <https://doi.org/10.3389/fmicb.2015.00745>.
- Pastore, G., Kaiser, K., Kernchen, S., Spohn, M., 2020. Microbial release of apatite- and goethite-bound phosphate in acidic forest soils. *Geoderma* 370, 114360. <https://doi.org/10.1016/j.geoderma.2020.114360>.
- Penn, J.C., Camberato, J., 2019. A critical review on soil chemical processes that control how soil pH affects phosphorus availability to plants. *Agriculture* 9 (6), 120. <https://doi.org/10.3390/agriculture9060120>.
- Pikovskaya, R.L., 1948. Mobilization of phosphorus in soil in connection with the vital activity of some microbial species. *Microbiologia* 17, 362–370.
- Prietzl, J., Klysubun, W., Werner, F., 2016. Speciation of phosphorus in temperate zone forest soils as assessed by combined wet-chemical fractionation and XANES spectroscopy. *Journal of Plant Nutrition and Soil Science* 179, 168–185. <https://doi.org/10.1002/jpln.201500472>.
- Qessaoui, R., Bouharrou, R., Furze, J.N., El Aalaoui, M., Akroud, H., Amarrague, A., Van Vaerenbergh, J., Tahzima, R., Mayad, E.H., Chebli, B., 2019. Applications of new rhizobacteria *Pseudomonas* isolates in agroecology via fundamental processes complementing plant growth. *Scientific Reports* 9, 12832. <https://doi.org/10.1038/s41598-019-49216-8>.
- Rogers, J., Bennett, P., 2004. Mineral stimulation of subsurface microorganisms: release of limiting nutrients from silicates. *Chemical Geology* 203, 91–108. <https://doi.org/10.1016/j.chemgeo.2003.09.001>.
- Sandroni, V., Smith, C., 2002. Microwave digestion of sludge, soil and sediment samples for metal analysis by inductively coupled plasma-atomic emission spectrometry. *Analytica Chimica Acta* 468, 335–344. [https://doi.org/10.1016/S0003-2670\(02\)00655-4](https://doi.org/10.1016/S0003-2670(02)00655-4).
- Sauer, M., Porro, D., Mattanovich, D., Branduardi, P., 2008. Microbial production of organic acids: expanding the markets. *Trends in Biotechnology* 26, 100–108. <https://doi.org/10.1016/j.tibtech.2007.11.006>.
- Schaller, J., Faucherre, S., Joss, H., Obst, M., Goeckede, M., Planer-Friedrich, B., Peiffer, S., Gilfedder, B., Elberling, B., 2019. Silicon increases the phosphorus availability of arctic soils. *Scientific Reports* 9, 449. <https://doi.org/10.1038/s41598-018-37104-6>.
- Schmidt, T., Rodrigues, J., von Mering, C., 2014. Ecological consistency of SSU rRNA-based operational taxonomic units at a global scale. *PLoS Computational Biology* 10, e1003594. <https://doi.org/10.1371/journal.pcbi.1003594>.
- Smits, M.M., Wallander, H., 2017. Role of mycorrhizal symbiosis in mineral weathering and nutrient mining from soil parent material. *Mycorrhizal Mediation of Soil* 3, 35–46. <https://doi.org/10.1016/B978-0-12-804312-7.00003-6>.
- Spohn, M., Kuzyakov, Y., 2013. Phosphorus mineralization can be driven by microbial need for carbon. *Soil Biology & Biochemistry* 61, 69–75. <https://doi.org/10.1016/j.soilbio.2013.02.013>.
- Spohn, M., Zeiig, I., Brucker, E., Widdig, M., Lacher, U., Aburto, F., 2020. Phosphorus solubilization in the rhizosphere in two saporites with contrasting phosphorus fractions. *Geoderma* 366, 114245. <https://doi.org/10.1016/j.geoderma.2020.114245>.
- Syers, J.K., Williams, J.D.H., Campbell, A.S., Walker, T.W., 1967. The significance of apatite inclusions in soil phosphorus studies. *Soil Science Society of America Journal* 31, 752–756. <https://doi.org/10.2136/sssaj1967.03615995003100060016x>.
- Sutra, L., Risede, J., Gardan, L., 2000. Isolation of fluorescent *Pseudomonas* from the rhizosphere of banana plants antagonistic towards root necrotic fungi. *Letters in Applied Microbiology* 4, 289–293. <https://doi.org/10.1046/j.1472-765x.2000.00816.x>.
- Sverdrup, H., 2009. Chemical weathering of soil minerals and the role of biological processes. *Fungal Biology Reviews* 23, 94–100. <https://doi.org/10.1016/j.fbr.2009.12.001>.
- Uroz, S., Kelly, L.C., Turpault, M.P., Lepleux, C., Frey-Klett, P., 2015. The mineralosphere concept: mineralogical control of the distribution and function of mineral-associated bacterial communities. *Trends in Microbiology* 23, 751–762. <https://doi.org/10.1016/j.tim.2015.10.004>.
- Uroz, S., Calvaruso, C., Turpault, M.P., Frey-Klett, P., 2009. Mineral weathering by bacteria: ecology, actors and mechanisms. *Trends in Microbiology* 17, 378–387. <https://doi.org/10.1016/j.tim.2009.05.004>.
- Vance, E.D., Brookes, P.C., Jenkinson, D.S., 1987. An extraction method for measuring soil microbial biomass C. *Soil Biology & Biochemistry* 19, 703–707. [https://doi.org/10.1016/0038-0717\(87\)90052-6](https://doi.org/10.1016/0038-0717(87)90052-6).
- Vandevivere, P., Welch, S.A., Ullman, W.J., Kirchman, D., 1994. Enhanced dissolution of silicate minerals by bacteria at near-neutral pH. *Microbial Ecology* 27, 241–251. <https://doi.org/10.1007/BF00182408>.
- Violante, A., Cazzolino, V., Perelomov, L., Caporale, A.G., Pigna, M., 2010. Mobility and bioavailability of heavy metals and metalloids in soil environments. *Journal of Soil Science and Plant Nutrition* 10, 268–292. <https://doi.org/10.4067/S0718-95162010000100005>.
- Vorhies, J., Gaines, R., 2009. Microbial dissolution of clay minerals as a source of iron and silica in marine sediments. *Nature Geoscience* 2, 221–225. <https://doi.org/10.1038/ngeo441>.
- Wang, Q., Wang, R.R., He, L.Y., Lu, J.J., 2014. Changes in weathering effectiveness and community of culturable mineral-weathering bacteria along a soil profile. *Biology and Fertility of Soils* 50, 1025–1034. <https://doi.org/10.1007/s00374-014-0924-9>.
- Wang, D., Xie, Y., Jaisi, D., Jin, Y., 2016. Effects of low-molecular-weight organic acids on the dissolution of hydroxyapatite nanoparticles. *Environmental Sciences: Nano* 3, 768–779. <https://doi.org/10.1039/C6EN00085A>.
- Welch, S.A., Ullman, W.J., 1993. The effect of organic acids on plagioclase dissolution rates and stoichiometry. *Geochimica et Cosmochimica Acta* 57, 2725–2736. [https://doi.org/10.1016/0016-7037\(93\)90386-B](https://doi.org/10.1016/0016-7037(93)90386-B).
- Welch, S.A., Taunton, A.E., Banfield, J.F., 2002. Effect of microorganisms and microbial metabolites on apatite dissolution. *Geomicrobiology Journal* 19, 343–367. <https://doi.org/10.1080/01490450290098414>.
- White, A.F., Brantley, S.L., 1995. Chemical weathering rates of silicate minerals. In: *Reviews in Mineralogy and Geochemistry*, 31, pp. 1–583. <https://doi.org/10.1515/9781501509650>.
- White, A.F., Brantley, S.L., 2003. The effect of time on the weathering of silicate minerals: why do weathering rates differ in the laboratory and field? *Chemical Geology* 202, 479–506. <https://doi.org/10.1016/j.chemgeo.2003.03.001>.
- White, A.F., 2003. Natural weathering rates of silicate minerals. *Treatise on Geochemistry* 5, 133–168. <https://doi.org/10.1016/B0-08-043751-6/05076-3>.

- Widdig, M., Schless, P.M., Weig, A.R., Guhr, A., Biederman, L.A., Borer, E.T., Crawley, M.J., Kirkman, K.P., Seabloom, E.W., Wragg, P.D., Spohn, M., 2019. Nitrogen and phosphorus additions alter the abundance of phosphorus-solubilizing bacteria and phosphatase activity in grassland soils. *Frontiers in Environmental Science* 7, 185. <https://doi.org/10.3389/fenvs.2019.00185>.
- Wolff-Boenisch, D., Gislason, S.R., Oelkers, E.H., 2006. The effect of crystallinity on dissolution rates and CO₂ consumption capacity of silicates. *Geochimica and Cosmochimica Acta* 70, 858–870. <https://doi.org/10.1016/j.gca.2005.10.016>.
- Yang, X., Post, W.M., 2011. Phosphorus transformations as a function of pedogenesis: a synthesis of soil phosphorus data using Hedley fractionation method. *Biogeosciences* 8, 2907–2916. <https://doi.org/10.5194/bg-8-2907-2011>.
- Zhu, F., Qu, L., Hong, X., Sun, X., 2011. Isolation and characterization of a phosphate solubilizing halophilic bacterium *Kushneria* sp. YCWA18 from Daqiao saltern on the coast of yellow sea of China. *Evidence-based Complementary and Alternative Medicine* 615032, 1–6. <https://doi.org/10.1155/2011/615032>.
- Zou, X., Binkley, D., Doxtader, K.G., 1992. A new method for estimating gross P mineralization and microbial P immobilization rates in soils. *Plant and Soil* 147, 243–250. <https://doi.org/10.1007/BF00029076>.